Shift-Scale Invariance
of Electromagnetic Radiation

Nikolay Smolyakov
National Research Center "Kurchatov Institute" Moscow,
Russia

1. Introduction

Electromagnetic radiation generated by relativistic beams in electron storage rings is of considerable current use. Today's third-generation synchrotron radiation facilities are designed with a number of straight sections to maximize the use of so-called insertion devices (wigglers and undulators). Wigglers and undulators are magnetic devices producing a spatially periodic (or slightly nonperiodic) field variation that cause a charged electron beam to emit electromagnetic radiation with special properties. A wiggler magnet is a succession of alternating polarity magnetic poles, each of which bends the electron beam through an angle large compared with the natural opening angle of the synchrotron radiation $1/\gamma$, where $\gamma = electron\ energy/mc^2$ is the electron reduced energy, see Fig. 1.
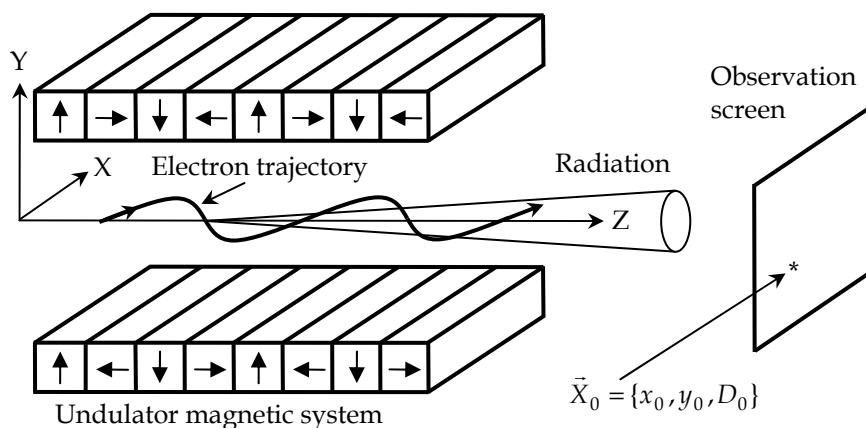

Fig. 1. Schematic of planar undulator and coordinate system. Arrows show magnetization directions.

Wigglers provide a strong magnetic field resulting in broadband emission of a fan-shaped beam of photons. Wiggler radiation is similar to standard synchrotron radiation produced by an individual bend magnet, but $2N$ times as intense due to $2N$ repetitive emission over

the length of a $2N$ pole wiggler. The design principle of undulator magnets is basically the same as of wiggler magnets. The difference comes from the magnetic field strength. Undulators, having relatively weak magnetic field, cause small beam deflection. In this case the photons emitted by an individual electron at the various poles in the magnet array interfere coherently. Due to the constructive interference, the undulator radiation beam's opening angle is reduced by $\sqrt{N}$ and thus radiation intensity from one electron per solid angle goes as N^2. A great body of publications is dedicated to undulator/wiggler radiation.

Over the last two decades considerable attention has been focused on the edge radiation as a bright source in infrared – ultraviolet spectral range. Edge radiation is produced when a relativistic charged particle passes through a region of rapid change of magnetic fields at the edges of storage ring bending magnets, see Fig. 2.
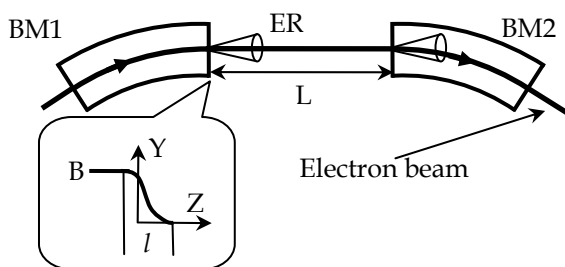

Fig. 2. Edge radiation setup: BM1, BM2 – bending magnets, ER – edge radiation, L – straight section length, l – length of the bending magnet fringe field.

It was discovered independently at the SPS proton synchrotron at CERN (Bossart et al., 1979, 1981) and the Tomsk electron synchrotron "Sirius" (Nikitin et al., 1980, 1981). Notice that the physics of edge radiation in proton storage rings (Coisson, 1979; Smolyakov, 1985, 1986) differs essentially from that in electron storage rings (Bessonov, 1981; Chubar & Smolyakov, 1993; Bosch, 1997; Geloni et al., 2009) though some similarities in their properties can be found. An important property of edge radiation from an electron beam is that its intensity substantially exceeds the standard synchrotron radiation intensity (from the regular bending magnetic field) in the long-wave spectral range, where its wavelength is much more than the corresponding synchrotron radiation critical wavelength. This feature has been confirmed experimentally (Shirasawa et al., 2003; Smolyakov & Hiraya, 2005).

The thorough simulations of radiation characteristics in real experiments call for the special-purpose computer codes. This chapter deals with the problem of how to calculate incoherent electromagnetic radiation, generated by a relativistic electron beam in external magnetic field.

Practically the measured magnetic field data, electron beam emittance, its energy spread, near-field effects (Hirai et al., 1984; Walker, 1988) as well as the finite width of the band-pass filter should be taken properly into account. We consider here the electron beam as an incoherent source, since it is assumed that electrons radiate independently from each other. Therefore, overall spectral intensity is determined by the sum of all the individual

intensities. Generally speaking, the spectral-angular distribution of energy radiated by one electron is dependent upon the following nine parameters: the electron initial transversal coordinates and velocities (both horizontal and vertical), its energy, radiation wavelength and the horizontal, vertical and longitudinal coordinates of the observation point. Let us briefly review numerical methods used for simulation of a single-electron spectrum.

It has been suggested that the ideal undulator has a perfect sinusoidal magnetic field, as with the planar (Alferov et al., 1976), helical (Alferov et al., 1976; Kincaid, 1977), elliptical (Yamamoto & Kitamura, 1987), two-harmonic (Dattoli & Voykov, 1993) and figura-8 (Tanaka & Kitamura, 1995) undulators. In this case, the spectral-angular density of undulator radiation in the far-field region involves a series of Bessel functions. This method is used in the computer codes SMUT (Jacobsen & Rarback, 1986; Rarback et al., 1988), URGENT (Walker, 1989; Walker & Diviacco, 1992) and US, which is incorporated into the software toolkit XOP (Sanchez del Rio & Dejus, 1998).

Radiation from an ideal undulator can also be calculated by going into a drift frame where an electron, on average, is at rest (Anacker et al., 1989). Both of these approaches have a fast speed of computation as their main advantage; however, they cannot be used for real undulators with imperfect magnetic fields, nor can they take into account near-field effects.

The most recently developed computer codes are able to use a real magnetic field map and, hence, compute the Fourier transformation of the radiation field numerically, using one of three ways. The spectral integrals may be evaluated by the saddle point method (Leubner & Ritsch, 1986a, 1986b; Steinmuller-Nethl et al., 1989). This method is used in the computer code RADID (C. Wang & Xian, 1990; C. Wang et al., 1994). This approach provides formulae similar to those for standard synchrotron radiation and, by its asymptotic nature, is applicable to insertion devices with strong magnetic fields (C. Wang & Jin, 1992; Walker, 1993). The second method involves the calculation of the radiation field in the time domain followed by the Fourier analysis in order to find the radiation spectrum. Such an approach, with minor modifications, is employed in the codes B2E (Elleaume & Marechal, 1991, 1997), UR (Dejus, 1994; Dejus & Luccio, 1994), YAUP (Boyanov et al., 1994) and SPECTRA (Tanaka & Kitamura, 2001) and is also integrated in the code RADID (C. Wang & Jin, 1992; C. Wang & Xiao, 1992; C. Wang, 1993). It gives direct insight into the physics of radiation and enables the calculation of radiation in a wide spectral range simultaneously, although requiring a huge amount of memory for angular distribution computation (Boyanov et al., 1994). The third method involves the direct integration of the Lienard-Wiechert retarded potentials in the frequency domain. This method is used in the computer codes SpontLight (Geisler et al., 1994), SRW (Chubar & Elleaume, 1998), SMARTWIG (Smolyakov, 2001), WAVE (Bahrdt et al., 2006) and in a number of others programs (Tatchyn et al., 1986; Chapman et al., 1989; Elleaume & Marechal, 1991, 1997; Ch. Wang et al., 1992; Yagi et al., 1995). The main problem of this approach comes from the fast oscillating factor in the integrand, requiring the use of extreme care in integration routines. Comparative studies of these algorithms can be found in (C. Wang & Jin, 1992; Dattoli et al., 1994).

Emittance effects are usually simulated by one of two ways: the Monte Carlo technique or the off-axis approximation method (Jacobsen & Rarback, 1986; Rarback et al., 1988), also known as the shift-invariant property of the radiation pattern (Chapman et al., 1989).

The Monte Carlo method, generally considered to be the most accurate, is employed in a number of computer codes, such as RADID (C. Wang & Xian, 1990; C. Wang & Jin, 1992; C. Wang & Xiao, 1992; C. Wang, 1993; C. Wang et al., 1994), UR (Dejus, 1994; Dejus & Luccio, 1994) and SpontLight (Geisler et al., 1994) (see also (Tatchyn et al., 1986; Yagi et al., 1995)). The problem with this approach is that the large number of individual computations for single-electron radiation can sometimes be too time consuming and impractical (Tatchyn et al., 1986; C. Wang, 1993; Lumpkin et al., 1995). Indeed, it needs generally the 5-dimantional sampling (two for electron position, two for electron deflection and one for its energy). It should be also mentioned that usually the simulations are carried out for a large number of observation points (or spectra). As a result, a total amount of individual simulations is huge.

The off-axis approximation method is based on the concept that spatial distributions of radiation from different electrons are essentially identical and are related to each other by the simple coordinate shifts arising due to angular and spatial electron spreads in the beam. If this is so, there is no need to compute the radiation for each electron separately and, hence, the computational task is simplified considerably. To our knowledge, paper (Nikitin & Epp, 1976) was the first to pioneer the application of this method. Owing to computational speed, this method is used extensively in a number of computer codes such as SMUT (Jacobsen & Rarback, 1986; Rarback et al., 1988), URGENT (Walker, 1989; Walker & Diviacco, 1992), B2E (Elleaume & Marechal, 1991, 1997), YAUP (Boyanov et al., 1994), US (Sanchez del Rio & Dejus, 1998), SRW (Chubar & Elleaume, 1998), SPECTRA (Tanaka & Kitamura, 2001) and SMARTWIG (Smolyakov, 2001) (see also (Anacker et al., 1989; Chapman et al., 1989; Ch. Wang et al., 1992)). The validity of the off-axis approximation method has, however, been proven in the far-field region only (Jacobsen & Rarback, 1986; Rarback et al., 1988; Chapman et al., 1989), since the equations controlling the pattern of radiation in the near-field region are rather cumbersome. Because of this, it has been argued that in a real-life geometry, when the distance to the observer is limited and does not tends to infinity, the radiation does not have the scale properties of standard synchrotron radiation (Chapman et al., 1989) and thus, the off-axis approximation method fails in the near-field region (C. Wang & Xiao, 1992; C. Wang, 1993). This point is particular important for edge radiation simulation (Chubar & Elleaume, 1998; Shirasawa et al., 2003; Smolyakov & Hiraya, 2005) since the straight section length usually is of the same order as the distance to the observer (edge radiation is generated by ultrarelativistic charged particles in the region of magnetic field change at bending magnets edges).

In fact, as it is demonstrated in this chapter, this statement is wrong. The off-axis approximation is valid in near-field region. It has been additionally proven in this chapter that electromagnetic radiation generated by relativistic particle in arbitrary transversal magnetic field (bending magnet fringe fields for edge radiation, undulator or wiggler field and so on) offers the radiation scale property. It means the following. The derived expressions clearly show that the electron energy does not appear explicitly in the formulas for radiation intensity distributions, but implicitly only, through a set of three new variables. These three variables can be called as reduced angles (horizontal and vertical) and reduced wavelength of radiation. By this is meant that the electron energy variation leads to variation of these listed above three reduced parameters only. These variations can be effectively reduced to the proper variations of observation point position and radiation wavelength. As a result, we can make the following statement. The variations of the eight of the nine parameters (usually the distance to observer is constant) can be reduced to the

correspondent variations of three parameters only: observation point position (horizontal and vertical) and radiation wavelength. This property simplifies considerably the simulation of electromagnetic radiation in a real situation. We did not employ any particular features of the external magnetic field in this study, except for taking the field to be uniform in the transversal directions. Therefore, the presented results are very general in nature.

We use the Gaussian unit system in this chapter.

2. Shift invariance of electron trajectories

Let us consider the motion of a single electron in the external transversal magnetic field $\vec{B}$. We choose the right-hand coordinate system in the usual fashion (Fig. 1): Z-axis is aligned with the electron beam propagation (straight section axis, undulator axis etc.), the X-axis is directed horizontally and the Y-axis is directed upwards. For simplicity the origin of the reference system is placed at the starting point of the magnetic field. In the vicinity of the Z-axis, the magnetic field can be approximated as:

$$\vec{B}(z) = \left\{ B_x(z), B_y(z), 0 \right\} \tag{1}$$

It follows from (1) that the magnetic field is presumed to be homogeneous in the transversal plane (i.e., its components do not depend on the coordinates x and y). The longitudinal component of the magnetic field B_z is ignored too. This means that the focusing properties of the undulator magnetic field are excluded from our analysis. This simplification is well suited for high-energy electron beams with relatively small transversal sizes and is a working standard for the simulation of spontaneous radiation. All the computer codes cited above in the introduction employ such approximations (or even a much higher degree of the undulator fields' idealization). Among the approximations that have been used in this study, the most radical limitations arise from expression (1). At the same time, there are no additional assumptions about the field profile so that its transversal components $B_{x,y}(z)$ can be considered to incorporate the correction fields at the ends of the undulator. These functions may also include magnetic system fabrication errors.

The electron motion in the magnetic field is governed by the Lorentz force equation:

$$\frac{d\vec{\beta}(t)}{dt} = \frac{e}{mc\gamma} \left[\vec{\beta}(t) \times \vec{B}(\vec{r}(t)) \right] \tag{2}$$

where c is the speed of light, e, m, $\vec{r}(t)$, $c\vec{\beta}(t)$ and γ are the electron's charge, mass, trajectory, velocity and reduced energy respectively: $\gamma = 1/\sqrt{1-\beta^2}$. We assume here that the radiated energy is negligible as compared to the electron kinetic energy, hence leaving γ constant. It readily follows from Eqs. (1) and (2) that:

$$\frac{d\beta_{x,y}(t)}{dt} = \frac{\pm Q}{\gamma} B_{y,x}(z(t)) \frac{dz(t)}{dt} \tag{3}$$

where $Q = (-e)/(mc^2)$. Remember, an electron has the negative charge so Q is positive. Since the magnetic field is given as a function of the longitudinal coordinate z, it is natural

to express the electron trajectory in terms of its longitudinal position as well. Integrating (3) with respect to time and using z as an independent variable instead of t, we get the following exact formulae:

$$\tilde{\beta}_x(z) = Q\int_0^z B_y(z')dz' \tag{4}$$

$$\tilde{\beta}_y(z) = -Q\int_0^z B_x(z')dz' \tag{5}$$

$$\beta_{x,y}(z) = \beta_{x,y}(0) + \frac{1}{\gamma}\tilde{\beta}_{x,y}(z) \tag{6}$$

$$\beta_z(z) = \sqrt{\beta^2 - \beta_x^{\;2}(z) - \beta_y^{\;2}(z)} \tag{7}$$

Similarly, we can now express the horizontal and vertical components of the electron trajectory $\vec{r}(z) = \{r_x(z), r_y(z), z\}$ as functions of its longitudinal position z:

$$r_{x,y}(z) = r_{x,y}(0) + \int_0^z \frac{\beta_{x,y}(z')}{\beta_z(z')}dz' \tag{8}$$

The time-dependence of the electron longitudinal position is implicitly governed by the equation:

$$t(z) = \int_0^z \frac{dz'}{c\beta_z(z')} \tag{9}$$

Let us suppose that the electron beam and the external magnetic field satisfy the following conditions:

i. The beam is relativistic with reduced energy $\gamma \gg 1$.
ii. The angular spread of the electron beam is small and the magnetic field slightly deflects an electron from its initial direction, i.e. $\left|\beta_{x,y}(z)\right| \ll 1$. For wiggler or undulator, this condition is equivalent to $K/\gamma \ll 1$, where K is the undulator deflection parameter.

Notice that this set of requirements is of a general nature and is fulfilled in practically all modern electron storage rings.

Expanding the function $\beta_z(z)$ in terms of the small quantities γ^{-2}, $\beta_{x,y}^2(z)$, we will get from (8) and (9):

$$r_{x,y}(z) = r_{x,y}(0) + \beta_{x,y}(0)\cdot z + \frac{1}{\gamma}\tilde{r}_{x,y}(z) \tag{10}$$

$$t(z) = \frac{z}{c}\left(1 + \frac{1}{2\gamma^2}\right) + \frac{1}{2c}\int_0^z \left(\beta_x^2(z') + \beta_y^2(z')\right)dz' \tag{11}$$

$$\tilde{r}_{x,y}(z) = \int_0^z \tilde{\beta}_{x,y}(z')dz' \tag{12}$$

Since the functions $\tilde{\beta}_{x,y}(z)$ and $\tilde{r}_{x,y}(z)$ are independent of the initial conditions $\beta_{x,y}(0)$, $r_{x,y}(0)$ and γ, they are the same for all electrons from the beam. The Eqs. (4) - (6), (10) - (12) express the electron trajectory in terms of the longitudinal coordinate z. These formulae relate all electron trajectories to a reference (ideal) orbit through a simple linear transformation, thus displaying the shift invariant property of electron trajectories. It is also important to note that the transversal components of the velocity, which are of fundamental importance to the density of electromagnetic radiation, are given by exact expressions. It should be noted that the simplicity of the equations defining the trajectory is a result of the fact that the magnetic field heterogeneity in transversal directions as well as its longitudinal component B_z are negligible. This leads to the separation of the problem into two independent equations, which can be integrated explicitly and independently from each other by the change of variables from t (time) to z (longitudinal position).

3. Spectral and angular distributions of radiations

Let us consider the radiation field of a moving electron, which is seen by the observer at time τ and at the observation point $\vec{X}_0$ with coordinates $\vec{X}_0 = \{x_0, y_0, D_0\}$. Notice that D_0 is the longitudinal distance between the starting point of the magnetic field and the observer, and is generally comparable to the magnetic field length L, although keeping in mind that $D_0 > L$. The electrical component of the radiation field is given by the following exact expression:

$$\vec{E}(\tau) = \frac{e}{cR(t)} \cdot \frac{[\vec{n}(t) \times [(\vec{n}(t) - \vec{\beta}(t)) \times \dot{\vec{\beta}}(t)]]}{(1 - (\vec{n}(t) \cdot \vec{\beta}(t)))^3} + \frac{e}{R^2(t)\gamma^2} \cdot \frac{\vec{n}(t) - \vec{\beta}(t)}{(1 - (\vec{n}(t) \cdot \vec{\beta}(t)))^3} \tag{13}$$

Here, the vector $\vec{R}(t) = \vec{X}_0 - \vec{r}(t)$ with absolute value $R(t)$ represents the distance between the emission point and the observer, the unit vector $\vec{n}(t) = \vec{R}(t)/R(t)$ points from the instantaneous position of the electron to the observer, and acceleration $c\dot{\vec{\beta}}(t)$ is calculated by Eq. (2). The quantities $\vec{n}(t)$, $\vec{\beta}(t)$, $\dot{\vec{\beta}}(t)$ and $R(t)$ on the right-hand side of Eq. (13) are to be evaluated at the retarded time t which must obey the equation:

$$c\tau = ct + R(t) \tag{14}$$

Differentiating the last relation, we find:

$$\frac{d\tau}{dt} = 1 - (\vec{n}(t) \cdot \vec{\beta}(t)) \tag{15}$$

Upon integrating (15) with respect to the retarded time we obtain the alternative relationship between observer time τ and retarded time t :

$$\tau(t) = \tau(0) + \int_0^t (1 - (\vec{n}(t') \cdot \vec{\beta}(t')))dt' \tag{16}$$

The first term in (13) arises from the electron acceleration and varies as R^{-1}. The second term in (13) is the so-called velocity field, which is independent of acceleration and essentially arises from static fields falling off as R^{-2}. At large distances this term is negligibly small and is often ignored. However in some cases of the long wavelength radiation simulation both terms in Eq. (13) should be considered (Roy et al., 2000). Thus we will include the velocity term into our analysis and furthermore will prove that its inclusion does not violate the shift-scale properties of radiation.

Let us consider the electromagnetic radiation with wavelength λ passing through an infinitesimal surface area ds located at the observation point $\vec{X}_0$ perpendicular to the Z-axis, as it shown in Fig. 1. The general expression for the number of photons $dN_{x,y}$ with horizontal (x) and vertical (y) polarization, emitted by one electron in its passage through the magnetic field per relative bandwidth $d\lambda/\lambda$ and per area ds can be written as follows:

$$dN_{x,y} = \frac{ds}{D_0^2}\left(\frac{d\lambda}{\lambda}\right)\frac{\alpha c^2 \gamma^2}{4\pi^2 e^2}\left|\tilde{E}_{x,y}(\lambda)\right|^2 \tag{17}$$

where α is the fine structure constant and $\tilde{E}_{x,y}(\lambda)$ is proportional to the Fourier-transform of the radiation field:

$$\tilde{E}_{x,y}(\lambda) = \frac{D_0}{\gamma}\int_{-\infty}^{\infty}\exp(i\frac{2\pi c}{\lambda}\tau)E_{x,y}(\tau)d\tau \tag{18}$$

A comprehensive study of electromagnetic radiation includes the simulation of its polarization, which is usually calculated via the Stokes parameters:

$$S_0 = A\left(\tilde{E}_x\tilde{E}_x^* + \tilde{E}_y\tilde{E}_y^*\right),$$
$$S_1 = A\left(\tilde{E}_x\tilde{E}_x^* - \tilde{E}_y\tilde{E}_y^*\right),$$
$$S_2 = A\left(\tilde{E}_x\tilde{E}_y^* + \tilde{E}_y\tilde{E}_x^*\right),$$
$$S_3 = -iA\left(\tilde{E}_x\tilde{E}_y^* - \tilde{E}_y\tilde{E}_x^*\right) \tag{19}$$

where

$$A = \frac{ds}{D_0^2}\left(\frac{d\lambda}{\lambda}\right)\frac{\alpha c^2 \gamma^2}{4\pi^2 e^2},$$

thus normalizing S_0 to the photon flux density (17).

One additional comment is necessary. The far-field approximation, which is extensively used in radiation simulations, implies that the distance between the source and the observer is vastly larger than the magnetic field length, so that the source of radiation is considered point-like. At this level of approximation, the variables $\vec{n}$ and R in (13) may be considered as constants, which uniquely determine the position of the observation point. The radiant energy in this case can be expressed conveniently in terms of angular coordinates of the observation point n_x and n_y. However, as it is shown in (Walker, 1988), the near-field effects that are caused by the finite distance to the observer can significantly change the properties of undulator radiation and hence should be properly taken into consideration. It means that the time-dependence of the unit vector $\vec{n}$ must be taken into account. That is why we specify the observer position by its Cartesian coordinates and consider the photon flux per small surface area rather than per a small solid angle.

In order to calculate the Fourier transform of the field in the frequency domain, we substitute the expressions (13) and (16) for electric field $\vec{E}(\tau)$ and observer time τ respectively, in Eq. (18). Furthermore, we change the variable of integration from retarded time t to the particle longitudinal coordinate z with the help of Eq. (9), thereby obtaining the following exact expression:

$$\tilde{E}_{x,y}(\lambda) = \frac{-2eQ}{c}\int_0^L \exp(i\Phi(z))\left(f_{x,y}(z)B_x(z) + g_{x,y}(z)B_y(z) - \frac{h_{x,y}(z)}{Q(D_0-z)}\right)\frac{D_0}{D_0-z}dz \ , \qquad (20)$$

$$\vec{f}(z) = \frac{[\vec{n}(z)\times[(\vec{n}(z)-\vec{\beta}(z))\times[\vec{\beta}(z)\times\vec{i}\,]]]}{2\gamma^2\beta_z(z)(1-(\vec{n}(z)\cdot\vec{\beta}(z)))^2}\cdot\frac{D_0-z}{R(z)} \ , \qquad (21)$$

$$\vec{g}(z) = \frac{[\vec{n}(z)\times[(\vec{n}(z)-\vec{\beta}(z))\times[\vec{\beta}(z)\times\vec{j}\,]]]}{2\gamma^2\beta_z(z)(1-(\vec{n}(z)\cdot\vec{\beta}(z)))^2}\cdot\frac{D_0-z}{R(z)} \ , \qquad (22)$$

$$\vec{h}(z) = \frac{\vec{n}(z)-\vec{\beta}(z)}{2\gamma^3\beta_z(z)(1-(\vec{n}(z)\cdot\vec{\beta}(z)))^2}\cdot\left(\frac{D_0-z}{R(z)}\right)^2 \ , \qquad (23)$$

$$\Phi(z) = \frac{2\pi c}{\lambda}\tau(0) + \frac{2\pi}{\lambda}\int_0^z(1-(\vec{n}(z')\cdot\vec{\beta}(z')))\frac{dz'}{\beta_z(z')} \ , \qquad (24)$$

where $\vec{i}$ and $\vec{j}$ are the unit vectors along the axis X and Y respectively. Since the first term $(2\pi c/\lambda)\tau(0)$ in phase (24) is z-independent, it can be dropped out because the constant phase factor leaves the physical quantities (17) and (19) unaltered.

It should be noted that in many papers the other expression is used instead of (20), see (Rarback et al., 1988; Chapman et al., 1989; Boyanov et al., 1994; Dattoli et al. 1994; Chubar & Elleaume, 1998; Tanaka & Kitamura, 2001). This expression has a more simple analytical form and can be derived from (20) as a result of integration by parts accompanied by the omitting of the boundary terms. It has been pointed out, however, that this simplification is not generally valid (Tatchyn et al., 1986) and ignoring the boundary terms may introduce

considerable errors in computer results (Walker, 1989). Thus we will use the expressions (20) - (24) here.

We will consider the radiation at small observation angles: $|n_x(z)| \ll 1$ and $|n_y(z)| \ll 1$. If so, let us expand R, n_z and β_z in power series of the small quantities γ^{-1}, $n_{x,y}$ and $\beta_{x,y}$:

$$R(z) = D_0 - z$$

$$n_z(z) = 1 - 0.5 \cdot (n_x^2(z) + n_y^2(z))$$

$$\beta_z(z) = 1 - 0.5 \cdot (\gamma^{-2} + \beta_x^2(z) + \beta_y^2(z))$$

Using these expansions and keeping only the leading terms, it is easily found that:

$$1 - (\vec{n} \cdot \vec{\beta}) = 0.5 \cdot \left(\gamma^{-2} + (n_x - \beta_x)^2 + (n_y - \beta_y)^2 \right) \tag{25}$$

Expanding the triple cross products in (21) and (22), using (25) and keeping again the leading terms, after a rather long computation we finally get:

$$f_x(z) = \left(\vec{f}(z) \cdot \vec{i} \right) = \frac{2 u_x(z) u_y(z)}{\left(1 + u_x^2(z) + u_y^2(z) \right)^2} \tag{26}$$

$$f_y(z) = \left(\vec{f}(z) \cdot \vec{j} \right) = \frac{1 + u_x^2(z) - u_y^2(z)}{\left(1 + u_x^2(z) + u_y^2(z) \right)^2} \tag{27}$$

$$g_x(z) = \left(\vec{g}(z) \cdot \vec{i} \right) = \frac{1 - u_x^2(z) + u_y^2(z)}{\left(1 + u_x^2(z) + u_y^2(z) \right)^2} \tag{28}$$

$$g_y(z) = \left(\vec{g}(z) \cdot \vec{j} \right) = -f_x(z) \tag{29}$$

$$h_{x,y}(z) = \frac{2 u_{x,y}(z)}{\left(1 + u_x^2(z) + u_y^2(z) \right)^2} \tag{30}$$

$$\Phi(z) = \frac{\pi}{\lambda \gamma^2} \int_0^z \left(1 + u_x^2(z') + u_y^2(z') \right) dz' \tag{31}$$

$$u_{x,y}(z) = \gamma n_{x,y}(z) - \gamma \beta_{x,y}(z) \tag{32}$$

The values of $f_{x,y}$, $g_{x,y}$ and $h_{x,y}$ are rapidly varying functions of the instantaneous electron angles $\beta_{x,y}(z)$ and the observation angles $n_{x,y}(z)$. The peak values are 0.25 for f_x and g_y, 1.0 for f_y and g_x, and $0.375\sqrt{3}$ for $h_{x,y}$. The values of these functions differ

noticeably from zero only within a small angle $\pm 1/\gamma$ from the electron velocity direction, which is common to electromagnetic radiation emitted by a relativistic charged particle. More detailed calculations show that correction terms for the expressions (26) - (31) are γ^2 times smaller than the leading terms and hence may be safely discarded.

All the functions $f_{x,y}(z)$, $g_{x,y}(z)$ and $h_{x,y}(z)$ in (20) are of the same order of magnitude and have a similar scale of variation. Thus the relative contribution of the velocity term $h_{x,y}(z)$ is determined by the ratio between magnetic field amplitude and factor $1/(QD_0)$. For an undulator with a sinusoidal magnetic field, the ratio is equal to $\lambda_w/(2\pi K D_0)$, where λ_w is the undulator period length and K is the undulator deflection parameter. Usually this quantity is negligibly small and thus the velocity term can be dropped out. However, at the level of approximation used in this paper, only those correction terms, which are proportional to the γ^{-2}, $n_{x,y}^2$ and $\beta_{x,y}^2$, are disregarded. Thus the velocity term has been retained here for generality.

4. Shift-scale invariance of radiation

Detailed theoretical investigations of electromagnetic radiation are certain to include simulation of radiation intensity for a great number of observation points and photon wavelengths. This means that we should repeat the individual calculations for a wide range of the following radiation's three parameters: its wavelength λ and transversal coordinates of the observation points x_0 and y_0. The longitudinal coordinates of the observation points D_0 are essentially the same since the observation plane is aligned perpendicularly to the Z-axis. To include the multi-electron effects into simulation, one must then repeat the calculation of single-electron radiation for a huge number of different electrons, each moving in its own trajectory. The trajectory is determined uniquely by the following five parameters: initial transversal positions of the electron $r_{x,y}(0)$, its initial angles $\beta_{x,y}(0)$ and its reduced energy γ. So, we have to compute single-electron radiation for a wide variety of values for each of just listed eight parameters by itself. Though this straightforward way is conceptually satisfying (and it is used in Monte-Carlo sampling), it is computationally formidable since the needed number of individual calculations is multiplicatively accumulated and the simulation quickly becomes too time consuming. That is why the reduction in number of independent variables is of fundamental importance.

Let us now proceed to analyze how the radiated fields $\tilde{E}_{x,y}$ are controlled by the following eight parameters: $r_{x,y}(0)$, $\beta_{x,y}(0)$, γ, x_o, y_o and λ. It should be noted that the radiated fields depend on these eight parameters only implicitly through the variable $\Lambda = \lambda\gamma^2$ and two functions, $u_x(z)$ and $u_y(z)$ (see Eqs. (20) and (26) - (31)).

In the case of small observation angles $\left|n_{x,y}(z)\right| \ll 1$, we can write:

$$n_x(z) = \frac{x_o - r_x(z)}{D_o - z} \tag{33}$$

$$n_y(z) = \frac{y_o - r_y(z)}{D_o - z} \tag{34}$$

By putting these relations and Eqs. (6) and (10) for the electron trajectory into Eqs. (32) for $u_x(z)$ and $u_y(z)$, we have after some simple algebraic manipulations:

$$u_{x,y}(z) = \Theta_{x,y} \frac{D_o}{D_o - z} - v_{x,y}(z) \tag{35}$$

$$v_{x,y}(z) = \frac{\tilde{r}_{x,y}(z)}{D_o - z} + \tilde{\beta}_{x,y}(z) \tag{36}$$

$$\theta_x = \frac{x_o - r_x(0)}{D_o} - \beta_x(0) \tag{37}$$

$$\theta_y = \frac{y_o - r_y(0)}{D_o} - \beta_y(0) \tag{38}$$

where $\Theta_{x,y} = \gamma\theta_{x,y}$. The quantities $\theta_{x,y}$ are the angles between the initial electron's velocity and the direction of observation. It is clear that the functions $v_{x,y}(z)$ are the same for all electrons in the beam being dependent only on the magnetic field $B_{x,y}(z)$ and longitudinal coordinate of the observation points D_o (see Eqs. (4), (5) and (12)). By substituting Eqs. (35) into the integral (31) and performing integration, we have:

$$\Phi(z) = \Phi_0(z) + \Phi_1(z), \tag{39}$$

$$\Phi_0(z) = \frac{\pi}{\Lambda}\left[z\left(1 + \Theta_x^2 + \Theta_y^2\right) - 2\Theta_x\tilde{r}_x(z) - 2\Theta_y\tilde{r}_y(z) + \int_0^z \left(\tilde{\beta}_x^2(z') + \tilde{\beta}_y^2(z')\right)dz' \right], \tag{40}$$

$$\Phi_1(z) = \frac{\pi}{\Lambda(D_o - z)}\left[\left(z\Theta_x - \tilde{r}_x(z)\right)^2 + \left(z\Theta_y - \tilde{r}_y(z)\right)^2 \right] \tag{41}$$

where $\Lambda = \lambda\gamma^2$. These three relations show explicitly that the phase $\Phi(z)$ depends on the electron initial parameters, its energy and radiation parameters only through the following four variables: $\Theta_{x,y}$, Λ and D_o. The first term in (39) is explicitly independent of D_o although implicitly it is D_o-dependent through the variables $\Theta_{x,y}$.

The foregoing allows us to express the main result of this study through the following compact relation:

$$\tilde{E}_{x,y}\left(r_x(0), r_y(0), \beta_x(0), \beta_y(0), \gamma, x_o, y_o, \lambda, D_o; \{B_x, B_y\}\right) = \tilde{E}_{x,y}\left(\Theta_x, \Theta_y, \Lambda, D_o; \{B_x, B_y\}\right) \tag{42}$$

where $\{B_x, B_y\}$ denotes the appropriate set of parameters, which uniquely determines the external magnetic field along. In the general case, this is an experimentally measured magnetic field mesh. For the case of ideal planar undulator with a sinusoidal field, it may be the following three parameters: number of the undulator periods, the length of period and magnetic field amplitude (or an undulator deflection parameter).

Expressions (37) and (38) for $\theta_{x,y}$ show explicitly that photon density (17) as well as the Stokes parameters (19) possess the shift-invariant property. It means that any changes in the electron initial parameters $r_{x,y}(0)$ and $\beta_{x,y}(0)$ may be reduced to the corresponding shift of the observer transversal coordinates x_o and y_o. Hence there is no need to repeatedly simulate the radiation from a great number of electrons with different trajectories. The desired radiation distribution for any electron can be obtained from the corresponding distribution of radiation that has been calculated for the electron with the same energy but following the equilibrium trajectory.

One can see from expression (42) that the functions $\tilde{E}_{x,y}$ are also scale-invariant relative to the reduced energy γ. Let us consider changing the electron energy $\gamma \to k\gamma$ such that the restriction $\gamma \gg 1$ remains intact. Such a change of energy results in the following variations of arguments: $\Lambda \to k^2\Lambda$ and $\Theta_{x,y} \to k\Theta_{x,y}$. These variations may be thought of as rescaling of the radiation wavelength $\lambda \to k^2\lambda$ and the observation angles $\theta_{x,y} \to k\theta_{x,y}$, which in turn can be boiled down to the corresponding shifts of the observer coordinates x_o and y_o. It means again that the simulation of radiation from electrons of differing energy may effectively be reduced to the simulation of radiation from a single electron with energy and trajectory in equilibrium, but with different radiation wavelengths and at different observation points.

It follows from the expressions (17) and (42) that photon density is also scale-invariant, which is to say that the number of photons is invariant under the following transformation:

$$\gamma \to k\gamma \,,$$
$$\theta_{x,y} \to k^{-1}\theta_{x,y} \,,$$
$$\lambda \to k^{-2}\lambda \,,$$
$$d\lambda \to k^{-2}d\lambda \,,$$
$$ds \to k^{-2}ds \tag{43}$$

These transformations leave the Stokes parameters also unchanged.

Since the parameters

$$\Theta_x = \gamma\theta_x = \gamma\left(\frac{x_o - r_x(0)}{D_o} - \beta_x(0)\right), \; \Theta_y = \gamma\theta_y = \gamma\left(\frac{y_o - r_y(0)}{D_o} - \beta_y(0)\right) \text{ and } \Lambda = \lambda\gamma^2$$

are of primary importance in describing the shift-scale invariant properties of electromagnetic radiation, we can call these variables "reduced angles" and "reduced wavelength" respectively.

Assuming the electron proceeds along an equilibrium trajectory which passes through the origin (i.e. $r_{x,y}(0) = 0$), the correction term $\Phi_1(z)$, which is primarily responsible for near-field effects, may be written as:

$$\Phi_1(z) = \frac{\pi}{\Lambda(D_o - z)}\left[\left(z\frac{\gamma x_o}{D_o} - \gamma r_x(z)\right)^2 + \left(z\frac{\gamma y_o}{D_o} - \gamma r_y(z)\right)^2\right] \tag{44}$$

For undulators with deflection parameter K and period length λ_w, the functions $\gamma r_{x,y}(z)$ oscillate with the amplitudes of the order of $K\lambda_w/(2\pi)$, what is typically much less than the undulator length L, which is the maximum value for z. If so, we can safely omit the terms $\gamma r_{x,y}(z)$ in (44). Let us consider the radiation at a large distance $D_o \gg L$, which enables us to substitute D_o for $(D_o - z)$ in (44). As a result, the phase term (44) can be approximated by:

$$\Phi_1(z) = \frac{\pi}{\lambda D_o^3}\left(x_o^2 + y_o^2\right)z^2 \tag{45}$$

This is in agreement with the correction term derived by (Walker, 1988).

To get the corresponding expressions in far-field approximation, we should proceed to limit $D_o \to \infty$, $x_o \to \infty$ and $y_o \to \infty$ while the ratios

$$x_o\big/D_o \quad \text{and} \quad y_o\big/D_o$$

are kept constant and become new transversal angular coordinates of the observation point. Then the ratio

$$ds\big/D_o^2$$

is turned to the infinitesimal solid angle $d\Omega$. In that event the initial transversal positions of the electron $r_{x,y}(0)$ are irrelevant and the correction term $\Phi_1(z)$ in (39) tends to zero.

It is notable that the shift-scale invariance of electromagnetic radiation, which is given by Eq. (42), is identical to those of standard synchrotron radiation. Indeed, the spectral – angular density of synchrotron radiation in far – field region depends on the ratio λ_c/λ, where $\lambda_c = 4\pi\rho/(3\gamma^3)$ is the critical wavelength and ρ is the bending radius. However, as Eq. (42) shows, bending magnetic field B_0 should appear in this ration explicitly, rather than implicitly through ρ. Using the relation $eB_0\rho = mc^2\gamma$, we get:

$$\frac{\lambda_c}{\lambda} = \frac{4\pi mc^2}{3eB_0}\frac{1}{\lambda\gamma^2} \tag{46}$$

thus displaying the Λ - dependence of synchrotron radiation spectra.

A comprehensive theoretical analysis of edge radiation in sharp-edge approximation has been recently done (Geloni et al., 2009). Sharp-edge approximation means that the magnetic field at the bending magnet edge has supposedly a stepwise change from its regular value B_0 to zero. In other words, the fringe field length $l = 0$, see Fig. 2. In this case we have two parameters completely defining the magnetic system: magnetic field amplitude B_0 and straight section length L, or $\{B_x, B_y\} = (B_0, L)$ in terms of Eq.(42). It has been shown analytically and verified numerically that in this case the edge radiation distributions have the property of similarity. Two dimensionless parameters

$$\delta \equiv \sqrt[3]{\frac{\rho^2 \lambda}{2\pi L^3}}$$

and

$$\phi \equiv \frac{2\pi L}{\lambda \gamma^2}$$

were defined, where ρ is the radius of the trajectory bend. The property of similarity means that data for different sets of edge radiation parameters corresponding to the same values of δ and ϕ reduce to a single curve when properly normalized (Geloni et al., 2009).

This result is in complete agreement with the shift-scale property of electromagnetic radiation presented here and furthermore, it is the particular case of the more general shift-scale property. As suggested by Eq. (42), in the sharp-edge approximation the Fourier-transform of the radiation field $\tilde{E}_{x,y}(\lambda)$ depends on six parameters, namely, two reduced angles Θ_x and Θ_y, reduced wavelength Λ, distance to the observation screen D_0, bending field amplitude B_0 and straight section length L. The use of parameter

$$\tilde{\rho} = \frac{mc^2}{eB_0}$$

with dimension of length rather than B_0 is more convenient for analysis. Since the electron charge e, its mass m and the speed of light c are the fundamental constants, the parameter $\tilde{\rho}$ is equivalent to B_0. By virtue of the relation $eB_0\rho = mc^2\gamma$, where ρ is the radius of the bend in the field B_0, we get: $\rho = \gamma\tilde{\rho}$. Radius of the trajectory bend ρ is much more convenient in practical use, but we should start our analysis with the parameter $\tilde{\rho}$ because it depends on B_0 only, while ρ depends both on B_0 and γ.

So, we can say that $\tilde{E}_{x,y}(\lambda)$ depends on the set of parameters

$$\left(\Theta_x, \Theta_y, \Lambda, \tilde{\rho}, D_0, L\right)$$

It is clear that the alternative set of the following parameters:

$$\left(\Theta_x, \Theta_y, \frac{2\pi L}{\Lambda}, \sqrt[3]{\frac{\tilde{\rho}^2 \Lambda}{2\pi L^3}}, D_0, L\right)$$

is mathematically equivalent to the previous one. Using the relations $\Lambda = \lambda\gamma^2$ and $\rho = \gamma\tilde{\rho}$, we get:

$$\frac{2\pi L}{\Lambda} = \frac{2\pi L}{\lambda\gamma^2} = \phi$$

and

$$\sqrt[3]{\frac{\tilde{\rho}^2 \Lambda}{2\pi L^3}} = \sqrt[3]{\frac{\rho^2 \lambda}{2\pi L^3}} = \delta ,$$

thus deriving the parameters φ and δ obtained by (Geloni et al., 2009) for the property of similarity.

5. Conclusion

The results of the theoretical analysis presented here show that electromagnetic radiation, generated by relativistic charged particles in external magnetic fields, offers shift-scale invariance properties which are analytically best expressed by the Eq. (42). It is significant to note that all previous analyses were based on assumptions which were very general in nature and the great bulk of insertion devices match these assumptions without any loss in generality. Let us list here the all constrains we have imposed.

A relativistic charged particle ($\gamma \gg 1$) has small transversal components of its reduced velocity: $\sqrt{\beta_x^2(z) + \beta_y^2(z)} \ll 1$. Electromagnetic radiation is observed at small angles: $\sqrt{n_x^2(z) + n_y^2(z)} \ll 1$. The external magnetic field is taken to be uniform in a transversal plane, and its longitudinal component is zero. This last requirement is the most essential one and there is no way of applying the results obtained here if the undulator focusing properties is to be included into consideration. In our study we did not consider any specific features of the external magnetic field such as its periodicity, etc. This means that any radiation, generated by relativistic charged particles in an external magnetic field under conditions just mentioned, is shift-scale invariant.

It is important that the Fourier-transform of the radiation field $\tilde{E}_{x,y}(\lambda)$ defined by Eq. (18) depends on the electron energy γ only implicitly, through the reduced angles $\Theta_{x,y}$ and reduced wavelength Λ, see Eq. 42. This fact is not evident at first glance because reduced energy γ is a dimensionless parameter and dimensional analysis cannot be applied here. In addition, the electron trajectory depends explicitly on its reduced energy γ while the dependence of the radiation field $E_{x,y}(\tau)$ on trajectory parameters is fairly intricate, see Eqs. (13), (20-24) (recall that the unit vector $\vec{n}(z)$ is trajectory-dependent).

The shift-scale property of electromagnetic radiation suggests the following elements in the algorithm for the simulation of radiation from an electron beam in a real-life experimental setup. With knowledge of external magnetic field (undulator field, fringe field at the ends of storage ring bending magnets and so on), it is possible to find four parameters $r_{x,y}(0)$ and $\beta_{x,y}(0)$, such that the electron with a mean energy is moving along the equilibrium trajectory. In particular, these parameters are zero if the correction fields are included in the undulator magnetic field map. For this single electron, we can compute the spectral-spatial distribution of radiation for a number of wavelengths λ and at different observation points x_o and y_o. With knowledge of this radiation distribution, the effects of electron beam emittance, its energy spread and finite width of the spectral device may be included in the simulation via numerical convolution. To do this would require no more than a three-dimensional integration.

For undulators with large number of periods $N \gg 1$, further simplifications can be made on the following qualitative grounds. The spectral width of the i-th harmonic is equal to

$$\Delta\lambda = \lambda\big/(iN),$$

which yields the corresponding range

$$\Delta\Lambda = \Lambda\big/(iN)$$

From this, it follows that variation in γ through the range

$$\Delta\gamma = \gamma\big/(2iN)$$

can radically alter the distribution of undulator radiation.

The cone of the i-th harmonic has the angular size

$$\theta_i = \frac{1}{\gamma}\sqrt{\frac{1+0.5K^2}{2iN}}$$

This means that the variables $\Theta_{x,y}$ change of the order of $\gamma\theta_i$ which will alter the undulator radiation distribution. On the other hand, $\Theta_{x,y}$ vary directly with the energy $\Delta\Theta_{x,y} = \Delta\gamma \cdot \theta_{x,y}$. We will consider the radiation not far from the undulator axis $\theta_{x,y} = \delta_{x,y} \cdot \theta_i$, where $\delta_{x,y}$ are of the order of 1. The following range for γ variation is thus

$$\Delta\gamma = \gamma\big/\delta_{x,y},$$

which is considerably more than

$$\gamma\big/(2iN)$$

This means that γ variation affects the spectral-angular distribution of undulator radiation much more through the resulting change in variable Λ rather than through $\Theta_{x,y}$. If this is so, when averaging the radiation distribution over the energy spread, we only need to consider the γ variation for the variable Λ and use the mean value of γ for the variables $\Theta_{x,y}$. As a result this averaging process can be reduced simply to the corresponding integration over the radiation wavelength λ.

The shift-scale invariance of radiation distributions can be effectively employed in the raytracing computer codes such as RAY (Erko et al., 2008). For more sophisticated analyses, based on wavefront propagation simulation (Erko et al., 2008), it has been necessary to amplify the results presented here by the proper studying of the term $(2\pi c/\lambda)\tau(0)$ in the phase (24). This term is z-independent, has no effect on the radiation intensity and thus it was eliminated from our analysis here. At the same time it depends on the observation point

and therefore plays an important role in wavefront propagation calculations. Such kind of theoretical analysis has been performed for the particular case of standard synchrotron radiation (Smolyakov, 1998). Some results of numerical simulations can be found in (Chubar et al., 1999), while the general case of radiation has yet to be analyzed.

6. References

Alferov, D.F.; Bashmakov, Yu.A. & Bessonov, E.G. (1976). Undulator radiation. *Proceedings (Trudy) of the P.N. Lebedev Physics Institute,* Vol.80, (1976), pp. 97-123, ISBN 0-306-10932-8, Consultants Bureau, New York

Anacker, D.C.; Hale, W. & Erskine, J.L. (1989). An algorithm for computer simulation of undulators and wigglers. *Nuclear Instruments and Methods in Physics Research A*, Vol.284, Nos.2-3, (December 1989), pp. 514-522, ISSN 0168-9002

Bahrdt, J; Scheer, M. & Wustefeld, G. (2006). Tracking simulations and dynamic multipole shimming for helical undulators. *Proceedings of the Tenth European Particle Accelerator Conference (EPAC'06)*, pp. 3562-3564, ISBN 92-9083-278-9, Edinburgh, UK, June 26-30, 2006

Bessonov, E.G. (1981). On a class of electromagnetic waves. *Soviet Physics – JETP,* Vol.53, No.3, (March 1981), pp. 433-436, ISSN 0038-5646

Bosch, R.A. (1997). Long-wavelength radiation along a straight-section axis in an electron storage ring. *Nuclear Instruments and Methods in Physics Research A*, Vol.386, Nos.2-3, (February 1997), pp. 525-530, ISSN 0168-9002

Bossart, R.; Bosser, J.; Burnod, L.; Coisson, R.; D'Amico, E.; Hofmann, A. & Mann, J. (1979). Observation of visible synchrotron radiation emitted by a high-energy proton beam at the edge of a magnetic field. *Nuclear Instruments and Methods*, Vol.164, No.2, (August 1979), pp. 375-380, ISSN 0029-554X

Bossart, R.; Bosser, J.; Burnod, L.; D'Amico, E.; Ferioli, G.; Mann, J. & Meot, F. (1981). Proton beam profile measurements with synchrotron light. *Nuclear Instruments and Methods*, Vol.184, Nos.2-3, (June 1981), pp. 349-357, ISSN 0029-554X

Boyanov, B.I.; Bunker, G.; Lee J. M. & Morrison T. I. (1994). Numerical modeling of tapered undulator. *Nuclear Instruments and Methods in Physics Research A*, Vol.339, No.3, (February 1994), pp. 596-603, ISSN 0168-9002

Chapman, K.; Lai, B.; Cerrina, F. & Viccaro, J. (1989). Modelling of undulator sources. *Nuclear Instruments and Methods in Physics Research A*, Vol.283, No.1, (October 1989), pp. 88-99, ISSN 0168-9002

Chubar, O.V. & Elleaume, P. (1998). Accurate and efficient computation of synchrotron radiation in the near field region. *Proceedings of the Sixth European Particle Accelerator Conference (EPAC'98)*, pp. 1177-1179, ISBN 0 7503 0579 7, Stockholm, Sweden, June 22-26, 1998

Chubar, O.V.; Elleaume, P. & Snigirev A. (1999). Phase analysis and focusing of synchrotron radiation. *Nuclear Instruments and Methods in Physics Research A*, Vol. 435, No.3, (October 1999), pp. 495-508, ISSN 0168-9002

Chubar, O.V. & Smolyakov, N.V. (1993). VUV range edge radiation in electron storage rings. *Journal of Optics (Paris)*, Vol.24, No.3, (May 1993), pp. 117-121 ISSN 0150-536X

Coisson, R. (1979). Angular-spectral distribution and polarization of synchrotron radiation from a « short » magnet. *Physical Review A – General Physics,* Vol.20, No.2, (August 1979), pp. 524-528, ISSN 0556-2791

Dattoli, G.; Giannessi L. & Voikov G. (1994). Analytical and numerical computation of undulator brightness: a comparison. *Computers & Mathematics with Applications,* Vol.27, No.6, (March 1994), pp. 63-78, ISSN 0898-1221

Dattoli, G. & Voykov, G. (1993). Spectral properties of two-harmonic undulator radiation. *Physical Review E,* Vol.48, No.4, (October 1993), pp. 3030-3039, ISSN 1539-3755

Dejus, R. J. (1994). Computer simulations of the wiggler spectrum. *Nuclear Instruments and Methods in Physics Research A*, Vol.347, Nos.1-3, (August 1994), pp. 56-60, ISSN 0168-9002

Dejus, R. J. & Luccio, A. (1994). Program UR: General purpose code for synchrotron radiation calculations. *Nuclear Instruments and Methods in Physics Research A*, Vol.347, Nos.1-3, (August 1994), pp. 61-66, ISSN 0168-9002

Elleaume, P. & Marechal, X. (1991). Polarization characteristics of various ID's. *Internal Report ESRF-SR/ID-91-47,* (February 1991)

Elleaume, P. & Marechal, X. (1997). B2E: A software to compute synchrotron radiation from magnetic field data. Version 1.0. *Internal Report ESRF-SR/ID-91-54,* (March 1997)

Erko, A.; Idir, M.; Krist, T. & Michette, A.G. (2008). *Modern Developments in X-Ray and Neutron Optics, Springer Series in Optical Sciences,* Vol. 137, Springer, ISBN 978-3-540-74560-0, Springer Berlin Heidelberg New York

Geisler, A.; Ridder M. & Schmidt, T. (1994). SpontLight: A package for synchrotron radiation calculations. *DELTA Internal Report 94-7,* (April 1994), University of Dortmund, Institute for Acceleratorphysics, 44221 Dortmund, Germany

Geloni, G.; Kocharyan, V.; Saldin, E.; Schneidmiller, E. & Yurkov, M. (2009). Theory of edge radiation. Part I: Foundations and basic applications. *Nuclear Instruments and Methods in Physics Research A*, Vol.605, No.3, (July 2009), pp. 409-429, ISSN 0168-9002

Hirai, Y.; Luccio, A. & Yu, L. (1984). Study of the radiation from an undulator: Near fielf formation. *Journal of Applied Physics,* Vol.55, No.1, (January 1984), pp. 25-32, ISSN 0021-8979

Jacobsen, C. & Rarback, H. (1986). Prediction on the performance of the soft X-ray undulator. *Proceedings of SPIE,* Vol. 582, (January 1986), pp. 201-212, ISBN 0-89252-617-3

Kincaid, B.M. (1977). A short-period helical wiggler as an improved source of synchrotron radiation. *Journal of Applied Physics,* Vol.48, No.7, (July 1977), pp. 2684-2691, ISSN 0021-8979

Leubner, C. & Ritsch, H. (1986a). Accurate emission spectra from planar strong field wigglers with arbitrary field variation. *Nuclear Instruments and Methods in Physics Research A*, Vol.246, Nos.1-3, (May 1986), pp. 45-49, ISSN 0168-9002

Leubner, C. & Ritsch, H. (1986b). A note on the uniform asymptotic expansion of integrals with coalescing endpoint and saddle points. *Journal of Physics A: Mathematical and General,* Vol.19, No.3, (February 1986), pp. 329-335, ISSN 0305-4470

Lumpkin, A.; Yang, B.; Chung, Y.; Dejus, R.; Voykov G. & Dattoli G. (1995). Preliminary calculations on the determination of APS particle-beam parameters based on undulator radiation. *Proceedings of the Sixteenth Particle Accelerator Conference (PAC'95)*, pp. 2598-2600, ISBN 0780329376, Dallas, Texas, US, May 1-5, 1995

Nikitin, M.M.; Medvedev, A.F. & Moiseev, M.B. (1981). Synchrotron radiation from ends of straight-linear interval. *IEEE Transactions on Nuclear Science*, Vol.NS-28, No.3, (June 1981), pp. 3130-3132, ISSN 0018-9499

Nikitin, M.M.; Medvedev, A.F.; Moiseev, M.B. & Epp, V.Ya. (1980). Interference of synchrotron radiation. *Soviet Physics – JETP,* Vol.52, No.3, (September 1980), pp. 388-394, ISSN 0038-5646

Nikitin, M.M. & Epp, V.Ya. (1976). Effect of beam parameters on undulator radiation. *Soviet Physics: Technical Physics,* Vol.21, No.11, (November 1976), pp.1404-1407, ISSN 0038-5662

Rarback, H.; Jacobsen, C.; Kirz, J. & McNulty, I. (1988). The performance of the NSLS mini-undulator. *Nuclear Instruments and Methods in Physics Research A*, Vol.266, Nos.1-3, (April 1988), pp. 96-105, ISSN 0168-9002

Roy, P.; Guidi Cestelli, M.; Nucara A.; Marcouille, O.; Calvani, P.; Giura, P.; Paolone, A.; Mathis, Y.-L. & Gerschel A. (2000). Spectral distribution of infrared synchrotron radiation by an insertion device and its edges: A comparison between experimental and simulated spectra. *Physical Review Letters,* Vol.84, No.3 (January 2000), pp. 483-486, ISSN 1079-7114

Sanchez del Rio, M. & Dejus, R.J. (1998). XOP: recent developments. *Proceedings of SPIE,* Vol. 3448, (December 1998), pp. 340-345, ISSN 0277-786X

Shirasawa, K.; Smolyakov, N.V.; Hiraya, A. & Muneyoshi, T. (2003). Edge radiation as IR-VUV source. *Nuclear Instruments and Methods in Physics Research B*, Vol.199, (January 2003), pp. 526-530, ISSN 0168-583X

Smolyakov, N.V. (1985). Interference accompanying radiation from protons in the fringe field of dipole magnets in a synchrotron. *Soviet Physics: Technical Physics,* Vol.30, No.3, (March 1985), pp.291-295, ISSN 0038-5662

Smolyakov, N.V. (1986). Electromagnetic radiation from protons in the edge fields of synchrotron dipole magnets. *Soviet Physics: Technical Physics,* Vol.31, No.7, (July 1986), pp.741-744, ISSN 0038-5662

Smolyakov, N.V. (1998). Wave-optical properties of synchrotron radiation. *Nuclear Instruments and Methods in Physics Research A*, Vol. 405, Nos.2-3, (March 1998), pp. 235-238, ISSN 0168-9002

Smolyakov, N.V. (2001). Shift-scale invariance based computer code for wiggler radiation simulation. *Nuclear Instruments and Methods in Physics Research A*, Vol. 467-468, No.1, (July 2001), pp. 210-212, ISSN 0168-9002

Smolyakov, N.V. & Hiraya, A. (2005). Study of edge radiation at HiSOR storage ring. *Nuclear Instruments and Methods in Physics Research A*, Vol.543, No.1, (May 2005), pp. 51-54, ISSN 0168-9002

Steinmuller-Nethl, D.; Steinmuller, D. & Leubner, C. (1989). Spectral and angular distribution of radiation from advanced wigglers with sharply peaked magnetic fields. *Nuclear Instruments and Methods in Physics Research A*, Vol.285, Nos.1-2, (December 1989), pp. 307-312, ISSN 0168-9002

Tanaka, T. & Kitamura, H. (1995). Figure-8 undulator as an insertion device with linear polarization and low on-axis power density. *Nuclear Instruments and Methods in Physics Research A*, Vol.364, No.2, (October 1995), pp. 368-373, ISSN 0168-9002

Tanaka, T. & Kitamura, H. (2001). SPECTRA: a synchrotron radiation calculating code. *Journal of Synchrotron Radiation,* Vol.8, No.6 (November 2001), pp. 1221-1228, ISSN 0909-0495

Tatchyn, R.; Cox, A. D. & Qadri S. (1986). Undulator spectra: Computer simulations and modeling. *Proceedings of SPIE,* Vol. 582, (January 1986), pp. 47-65, ISBN 0-89252-617-3

Walker, R.P. (1988). Near field effects in off-axis undulator radiation. *Nuclear Instruments and Methods in Physics Research A*, Vol.267, Nos.2-3, (May 1988), pp. 537-546, ISSN 0168-9002

Walker, R.P. (1989). Calculation of undulator radiation spectral and angular distributions. *Review of Scientific Instruments,* Vol.60, No.7, (July 1989), pp. 1816-1819, ISSN 0034-6748

Walker, R.P. (1993). Interference effects in undulator and wiggler radiation sources. *Nuclear Instruments and Methods in Physics Research A*, Vol.335, Nos.1-2, (October 1993), pp. 328-337, ISSN 0168-9002

Walker, R.P. & Diviacco, B. (1992). URGENT – A computer program for calculating undulator radiation spectral, angular, polarization, and power density properties. *Review of Scientific Instruments,* Vol.63, No.1, (January 1992), pp. 392-395, ISSN 0034-6748

Wang, C. (1993). Monte Carlo calculation of multi-electron effects on synchrotron radiation. *Proceedings of SPIE,* Vol. 2013, (November 1993), pp. 126-137, ISBN 9780819412621

Wang, C. & Jin, Y. (1992) Undulator properties calculated with RADID. *Proceedings of the International Conference on Synchrotron Radiation Sources,* pp. 264-269, Indore, India, February 3-6, 1992

Wang, C.; Schlueter, R.; Hoyer E. & Heimann, P. (1994). Design of the advanced light source elliptical wiggler. *Nuclear Instruments and Methods in Physics Research A*, Vol.347, Nos.1-3, (August 1994), pp. 67-72, ISSN 0168-9002

Wang, C. & Xian, D. (1990). Radid: A software for insertion device radiation calculation. *Nuclear Instruments and Methods in Physics Research A*, Vol.288, Nos.2-3, (March 1990), pp. 649-658, ISSN 0168-9002

Wang, C. & Xiao, Y. (1992). On algorithms for undulator radiation calculation. *Proceedings of the International Conference on Synchrotron Radiation Sources,* pp. 270-277, Indore, India, February 3-6, 1992

Wang, Ch.; Molter, K.; Bahrdt, J.; Gaupp, A.; Peatman, W.B.; Ulm, G. & Wende, B. (1992). Calculation of undulator radiation from measured magnetic fields and comparison with measured spectra. *Proceedings of the Third European Particle Accelerator Conference (EPAC'92)*, Vol.2, pp. 928-930, ISBN 2-86332-115-3, Berlin, Germany, March 24-28, 1992

Yagi, K.; Yuri, M.; Sugiyama, S. & Onuki, H. (1995). Computer simulation study of undulator radiation. *Review of Scientific Instruments,* Vol.66, No.2, (February 1995), pp. 1993-1995, ISSN 0034-6748

Yamamoto, S. & Kitamura, H. (1987). Generation of quasi-circularly polarized undulator radiation with higher harmonics. *Japanese Journal of Applied Physics,* Vol.26, No.10, (October 1987), pp. L1613-L1615, ISSN 0021-4922
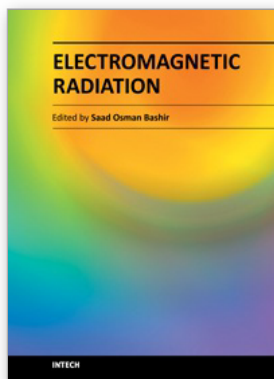
Electromagnetic Radiation

Edited by Prof. S. O. Bashir

The application of electromagnetic radiation in modern life is one of the most developing technologies. In this timely book, the authors comprehensively treat two integrated aspects of electromagnetic radiation, theory and application. It covers a wide scope of practical topics, including medical treatment, telecommunication systems, and radiation effects. The book sections have clear presentation, some state of the art examples, which makes this book an indispensable reference book for electromagnetic radiation applications.

How to reference

In order to correctly reference this scholarly work, feel free to copy and paste the following:

INTECH
open science | open minds